Contrib. Mineral. Petrol. 68, 151–169 (1979)

Contributions to Mineralogy and Petrology

A Geochemical Study of Magmatism Associated With the Initial Stages of Back-Arc Spreading

The Quaternary Volcanics of Bransfield Strait, From South Shetland Islands

Stephen D. Weaver,[1, 3] Andrew D. Saunders[1], Robert J. Pankhurst[2], and John Tarney[1]

[1] Department of Geological Sciences, University of Birmingham, Birmingham B15 2TT, Great Britain
[2] British Antarctic Survey, c/o Geochemical Division, Institute of Geological Sciences, 64–78 Gray's Inn Road, London WC1X 8NG, Great Britain
[3] Now at Department of Geology, University of Canterbury, Christchurch 1, New Zealand

Abstract. Bransfield Strait is a narrow basin separating the South Shetland Islands from the Antarctic Peninsula and is attributed to recent back-arc extension behind the South Shetland volcanic arc. The volcanic islands of Deception and Bridgeman are situated close to the axis of spreading, whereas Penguin Island lies slightly to the north of this axis. The mineralogy, petrology and geochemistry of the lavas of the three volcanoes have been studied in order to provide information on the nature of magmatism associated with the initial stages of back-arc spreading.

Deception Island lavas range from olivine basalt to dacite, and all are highly sodic, with high Na/K, K/Rb, Ba/Rb and Zr/Nb ratios and with $Ce_N/Yb_N = 2$. Incompatible elements increase systematically between basalt and rhyodacite, while Sr decreases, suggesting that fractional crystallisation is the dominant process relating lava compositions. The rhyodacites have high concentrations of Zr, Y and the REE and negative Eu anomalies and are compositionally similar to oceanic plagiogranite. Bridgeman Island lavas are mostly basaltic andesites, but the levels of many incompatible elements, including REE, are significantly lower than those of Deception lavas, although Ce_N/Yb_N ratios and $^{87}Sr/^{86}Sr$ ratios (0.7035) are the same. Penguin Island lavas are magnesian, mildly alkaline olivine basalts with a small range of composition that can be accommodated by fractional crystallisation of olivine, clinopyroxene and/or chromite. Penguin lavas have higher $^{87}Sr/^{86}Sr$ (0.7039) and Ce_N/Yb_N (4) ratios than Deception and Bridgeman lavas. The Rb/Sr ratios of Deception and Penguin basalts (ca. 0.01) are much too low to account for their present $^{87}Sr/^{86}Sr$ ratios.

Modelling suggests that the source regions of the lavas of the three volcanoes share many geochemical features, but there are also some significant differences, which probably reflects the complex nature of the mantle under an active island arc combined with complex melting relationships attending the initial stages of back-arc spreading. Favoured models suggest that Bridgeman lavas represent 10–20% melting and the more primitive Deception lavas 5–10% melting of spinel-peridotite, whereas Penguin lavas represent less then 5% melting of a garnet-peridotite source. The mantle source for Bridgeman lavas seems to have undergone short-term enrichment in K, Rb and Ba, possibly resulting from dewatering of the subducted slab. Hydrous melting conditions may also account for the more siliceous, high-alumina nature and low trace element contents of Bridgeman lavas.

1. Introduction

The magmatic record of Pacific ocean crust subduction along the west coast of the Antarctic Peninsula extends at least as far back as the lower Jurassic. Magmatism persisted until mid-Tertiary times when, following consumption of the Aluk Ridge (Herron and Tucholke, 1976), subduction ceased along most of the Peninsula as the south-east Pacific and the Antarctic became coupled to form a single Antarctic plate (Hayes and Ewing, 1970). Only ocean crust north-west of the South Shetland Islands continued to subduct throughout the late-Tertiary (Barker and Griffiths, 1972) and this consumption has now ceased. Volcanic activity still persists however behind the South Shetland island arc and the active and recently active volcanoes of Deception, Bridgeman and Penguin Islands appear to represent the surface expression of back-arc extension which has produced the narrow marginal basin of Bransfield Strait.

1.1. Tectonics and Structure of Bransfield Strait

The opening of the Scotia Sea (Fig. 1) is considered to be an essentially Tertiary event (Barker and Grif-

0010-7999/79/0068/0151/$03.80

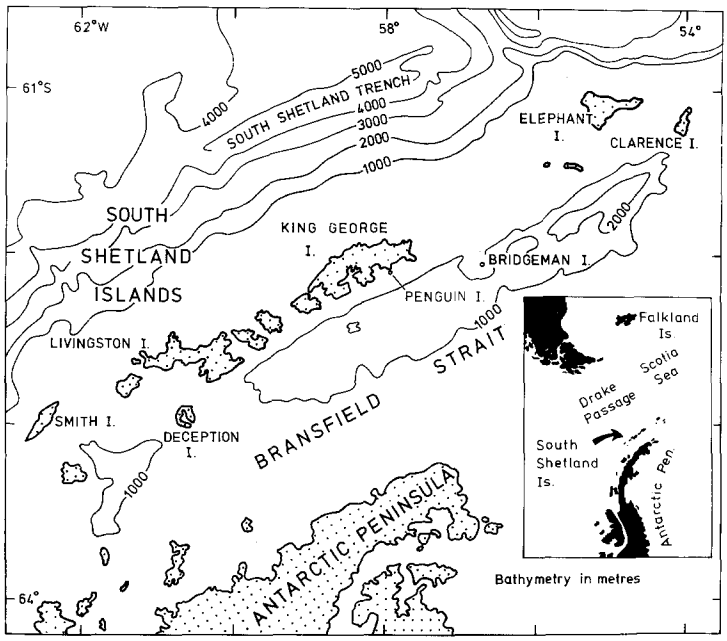

Fig. 1. Bathymetric map of the South Shetland Islands and Bransfield Strait

fiths, 1972; Barker, 1976) and involved spreading in Drake Passage from about 29 Ma ago (Barker and Burrell, 1977). West of the Shackleton Fracture Zone, late-Tertiary magnetic lineations parallel the line of the South Shetland Islands block, which lies off the tip of the Antarctic Peninsula at the western extremity of the South Scotia Ridge.

The South Shetland Islands from King George to Livingston Island constitute a narrow sialic crustal block bounded to the north-west by the South Shetland trench and to the south-east by Bransfield Strait (Fig. 1). Three spreading sections of ocean crust with ages ranging from at least 20 to 4 Ma have been identified north-west of the South Shetlands. Magnetic lineations give a full spreading rate of about 54 mm/year but about 4 Ma ago the rate slowed to only 5 mm/year (Barker, 1976). The South Shetland trench is now partially buried and appears to be seismically inactive.

The 65 km-wide Bransfield Strait has an asymmetric graben-like structure, bounded by normal faults (Ashcroft, 1972). It contains a narrow trough 2 km deep along which runs a line of seamounts from Deception Island to Bridgeman Island and beyond. The recent volcano of Penguin Island lies off this axis and is situated on the north-west, fault-controlled edge of the trough (Fig. 1). The crustal structure of Bransfield Strait, determined from seismic refraction studies (Ashcroft, 1972) shows high velocity (6.5–6.9 km/s) crustal material occurring only 5–6 km below the trough and the presence of anomalous mantle (7.6–7.7 km/s) at a depth of only 14 km. The seismic section resembles that of an oceanic axial zone, but with a thicker main crustal layer (Barker, 1976).

Bransfield Strait therefore appears to have been formed by crustal extension behind the South Shetland Islands, and the volcanic activity along the axis of Bransfield Strait suggests that some form of spreading is currently taking place. In spite of the fact that subduction at the South Shetlands trench may have reduced significantly 4 Ma ago, it is likely that the back-arc extension is causally related to subduction. Magnetic lineation data indicate that extension began between 1 and 2 Ma ago (Roach and Griffiths, pers. comm.) There is thus no doubt that Bransfield Strait is geologically very young and currently active and it has been likened (Barker and Griffiths, 1972; Davey, 1972) to the marginal basins of the Western Pacific (Karig, 1971). The volcanoes of Deception, Bridgeman and Penguin Islands should therefore provide an opportunity to study the geochemistry of magmas produced at the inception of back-arc spreading.

2. Geology of the Volcanic Islands

2.1. Deception Island

Deception (62°57′S, 60°38′W) is the best known of the South Shetland Islands and has received considerable attention from geologists following the eruptions of 1967, 1969 and 1970. It is a composite stratovolcano 13.5 km in diameter and reaching a maximum height of 542 m (Fig. 2).

The geology of Deception Island is described by Hawkes (1961) and Gonzalez-Ferran and Katsui (1970). A comprehensive account of the volcanic evolution of the island is given by Baker et al.

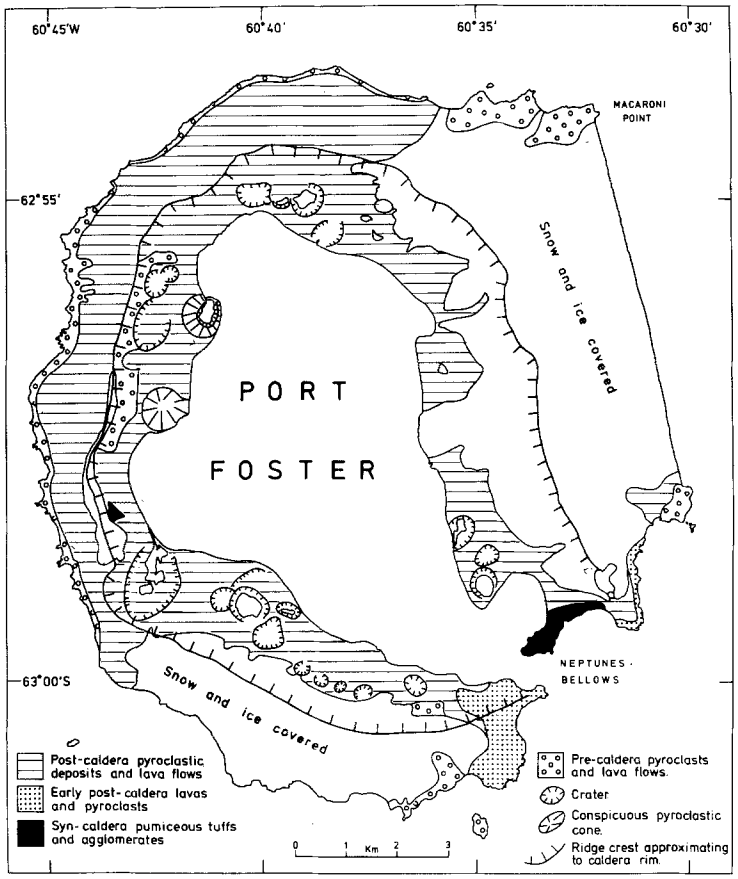

Fig. 2. Geological map of Deception Island, simplified after Baker et al. (1975)

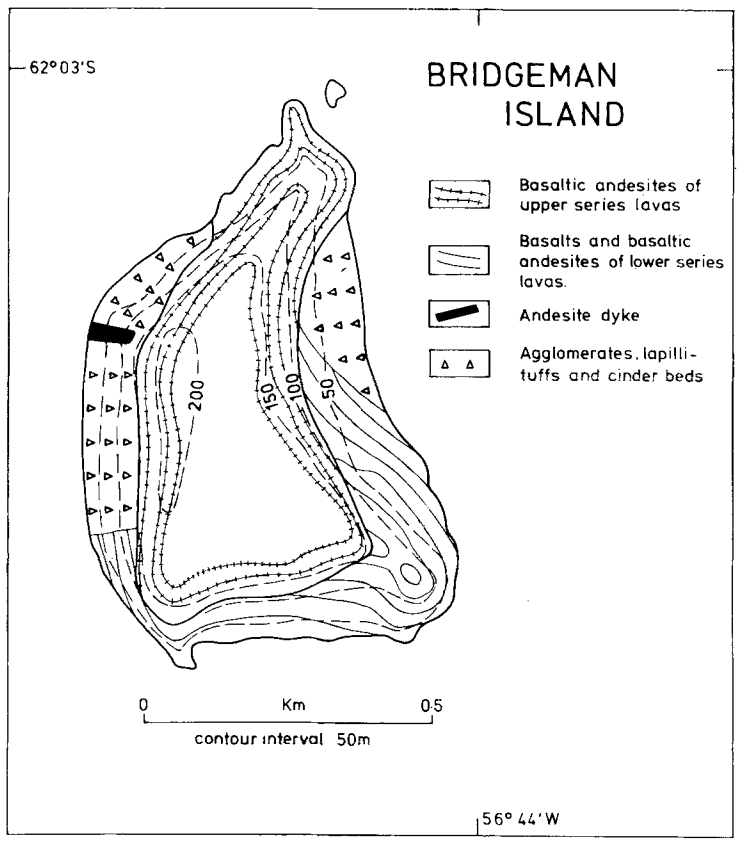

Fig. 3. Geological map of Bridgeman Island, with minor modifications after Gonzalez-Ferran and Katsui (1970)

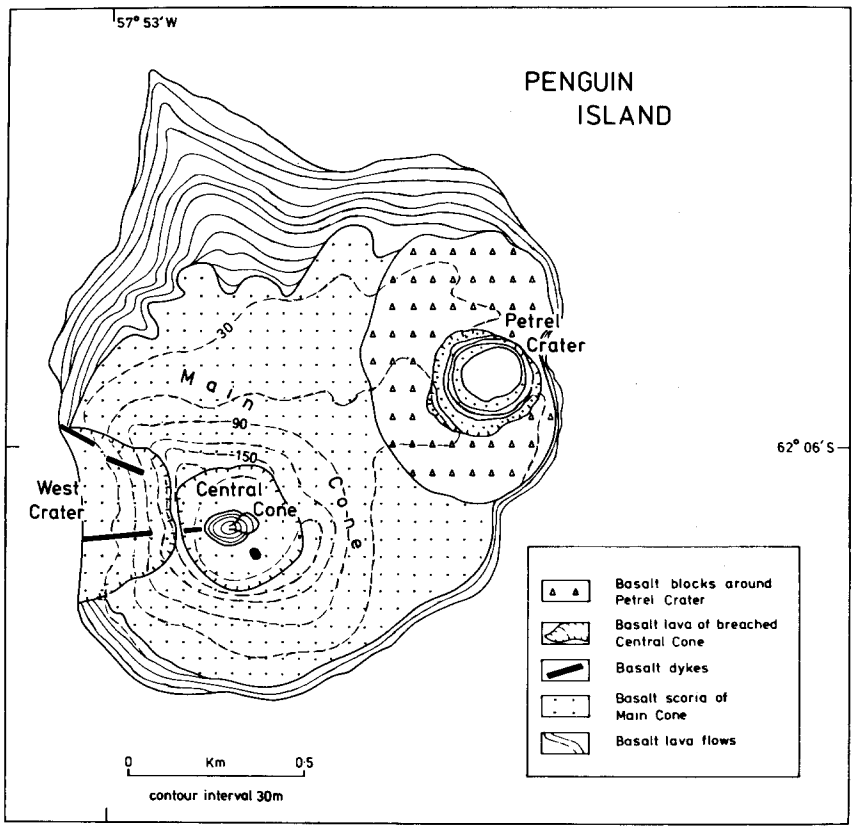

Fig. 4. Geological map of Penguin Island, with minor modifications after Gonzalez-Ferran and Katsui (1970)

(1975). The volcanic deposits may be ascribed to pre- and post-caldera events but some pyroclastic-flow deposits are regarded as syn-caldera (Baker et al., 1975), just preceding collapse. Pyroclastic deposits predominate and lavas account for 10–20% of the exposed portion of the volcano. The pre-caldera pyroclastic rocks and lavas are mainly basaltic. Post-caldera eruptive products are distinctly more silicic and include dacites. Although there appears to be a general trend towards more evolved, acid compositions with time, it is notable that basaltic magma was available throughout the history of the volcano.

2.2 Bridgeman Island

Bridgeman Island (62°03′S, 56°45′W) measures 900 m by 600 m and reaches a maximum height of 240 m (Fig. 3). The island is the remnant of a much larger volcanic edifice, eroded and now submerged beneath the sea. Bridgeman Island is geologically recent and its geomorphology and state of erosion are reminiscent of the Neptunes Bellows Group of Deception Island. Most of the pyroclastic deposits on Bridgeman are a bright brick-red colour owing to intense hydrothermal activity. Active fumaroles were reported on the island between 1821 and 1850 (Gonzalez-Ferran and Katsui, 1970).

The volcanic rocks may be divided into an upper series consisting predominantly of lavas and mantling an older series of lavas and pyroclastic deposits. The older series volcanics probably represent the deposits of a small scoria cone, disrupted and capped by lava flows. The younger volcanics were deposited on a very irregular surface with marked unconformity. Coarse pyroclasts filled in surface irregularities to some extent before the extrusion of a number of thick flows of basaltic andesite.

2.3. Penguin Island

Penguin Island (62°06′S, 57°56′W), located on the south side of King George Island, is about 1.7 km in diameter and is dominated by the regular uneroded slopes of a basalt scoria cone rising to 180 m above sea level and situated upon a 20 m-high platform composed of basaltic lava flows (Fig. 4). The lavas are dark to light grey microvesicular rocks containing abundant fresh, green olivine and dark, irridescent, pyroxene phenocrysts.

The volcanic morphology and unconsolidated nature of the pyroclastic deposits suggest that Penguin Island was active in historical times. Contained within the main crater is a secondary cone about 90 m across, breached on its east side by a flow of scoriaceous basalt, while on the west side of the main cone half of another explosion crater is preserved. Petrel Crater, on the east side of the island, is a neat circular crater surrounded by coarse blocks of basaltic lava thrown out in the explosion which formed it.

3. Petrography of the Lavas

3.1. Deception Island

Deception lavas range from olivine-basalts, basaltic andesites and andesites to dacites. The basaltic rocks are rich in modal plagioclase and usually contain 5–10% phenocrysts, but aphyric varieties do occur. Zoned bytownite phenocrysts predominate over olivine and diopsidic augite. The presence of Ca-poor clinopyroxene phenocrysts, identified optically by Hawkes (1961) and Baker et al. (1975), has not been confirmed by microprobe. Orthopyroxene is notably absent from the basaltic lavas. Basalts have intergranular

or intersertal textures and groundmasses composed of intermediate plagioclase, clinopyroxene (augite and pigeonite), olivine and titanomagnetite. Basaltic andesites have phenocrysts of labradorite, augite and minor orthopyroxene but olivine is either very sparse or absent from these rocks. Andesites and low-silica dacites are moderately porphyritic and have intersertal or intergranular textures. Phenocrysts are of andesine, augite and olivine together with rare microphenocrysts of hypersthene. The high-silica dacites and rhyodacites are strongly porphyritic rocks containing up to 20% phenocrysts and having trachytic and hyaline textures. Plagioclase of oligoclase composition predominates but phenocrysts and microphenocrysts of hypersthene, augite, fayalitic olivine and opaque ore are common.

3.2. Bridgeman Island

The lavas of Bridgeman Island are highly porphyritic basalts and basaltic andesites, containing 20–35% phenocrysts by volume. Typically, 15–25% are zoned calcic plagioclase phenocrysts, 5–10% are diopside and 0–10% are rounded or embayed olivine crystals. Rare bronzite cores in diopside phenocrysts have been identified by microprobe analysis. The groundmasses are highly feldspathic, have intergranular textures and are composed of plagioclase, clinopyroxene, little or no olivine, and opaque ore.

3.3. Penguin Island

Penguin Island lavas are all porphyritic olivine-basalts. Olivine phenocrysts comprise 5–15% and clinopyroxenes of diopsidic augite-salite composition 0–10%. Chromite occurs both as small crystals contained in olivine phenocrysts and as microphenocrysts. In the more chemically evolved rocks (Mg-poor), calcic plagioclase is present as microphenocrysts which have a seriate gradation into the groundmass.

4. Phenocryst Mineral Chemistry

The chemical mineralogy of the phenocrysts present in the Deception, Bridgeman and Penguin lavas was investigated using the Microscan 5 electron microprobe at Leicester University.

4.1. Olivine

(a) Deception Island. Small olivine phenocrysts occur in Deception Island basalts. Those in B138.2, a high-magnesian variety, have compositions in the range Fo_{83-80}. Optical determinations suggest that less forsteritic olivine of composition approaching Fo_{70} occurs in some of the basalts and, more rarely, in basaltic andesites. Andesite lavas have small olivine phenocrysts and compositions in the range Fo_{56-53} have been determined in a typical sample (B184.2). Microphenocrysts of distinctly fayalitic olivine occur in the dacites. Olivines in dacite B111.3 are of composition Fo_{37-36}. Optical determinations suggest that olivines as iron-rich as Fo_{20} are present in some of the dacites and rhyolites. More forsteritic olivine (Fo_{90}) than that identified in the lavas has been reported from gabbroic cumulate blocks by Baker et al. (1975).

(b) Bridgeman Island. A total range of composition of Fo_{87-78} has been measured on olivine phenocrysts in a single sample (P640.1b) of basalt from Bridgeman Island.

(c) Penguin Island. The total range of olivine phenocryst compositions measured is Fo_{88-79}. Individual phenocrysts are chemically zoned having Mg-rich cores and slightly more Fe-rich rims. The maximum range of composition encountered in a single crystal was Fo_{88-79} in a low-magnesian basalt (P810.4). Within the range Fo_{88-84}, olivine phenocrysts show a limited but distinct trend of Ca enrichment from 0.17 wt% to 0.24 wt%. This may be interpreted as a response to decreasing pressure during crystallization (Stormer, 1973). There is no increase in Ca content in the range Fo_{84-79} presumably reflecting crystallization under stable pressure conditions.

4.2. Pyroxenes

(a) Deception Island. Deception basalts contain a single, phenocryst pyroxene of average composition $Ca_{42}\ Mg_{46}\ Fe_{12}$. The average clinopyroxene composition in the low-silica andesites is $Ca_{41}\ Mg_{40}\ Fe_{19}$. In dacites, a clinopyroxene of composition $Ca_{40}\ Mg_{36}\ Fe_{24}$ is typical and is accompanied by separate phenocrysts of hypersthene of composition En_{52}. Olivine microphenocrysts of composition Fo_{37-36} have notably higher Fe/Mg ratios than coexisting hypersthenes and augites (Fig. 5). The microprobe data coupled with optical observation on Deception Island clinopyroxenes suggest that they form a continuous chemical series augite to ferroaugite in the range $Ca_{43}\ Mg_{46}\ Fe_{11}$ to $Ca_{39}\ Mg_{36}\ Fe_{25}$. This trend (Fig. 5) is similar to that for clinopyroxenes from Santorini (Nicholls, 1971) and not unlike the magnesian portion of the Thingmuli trend (Carmichael, 1964).

(b) Bridgeman Island. Basaltic lavas on Bridgeman Island contain phenocrysts of diopside of average composition $Ca_{47}\ Mg_{47}\ Fe_{6}$. The pyroxenes exhibit only limited chemical zoning, crystal rims attaining the composition $Ca_{43}\ Mg_{46}\ Fe_{11}$. Rarely, orthopyroxene cores in diopside can be identified; a single analysed core was bronzite of composition En_{79}.

(c) Penguin Island. Clinopyroxene phenocrysts in Penguin Island basalts range from diopsidic augite of composition $Ca_{43}\ Mg_{47}\ Fe_{10}$ to salite of composition $Ca_{47}\ Mg_{41}\ Fe_{12}$. Chemically zoned pyroxenes in the Mg-rich basalts have cores of diopsidic augite and rims of salite. Mg-poor basalts have phenocrysts of salite which have little zoning. The pyroxenes contain appreciable amounts of Ti and Al and have high Al_z contents reflecting the relatively low Si activity (undersaturation) of the Penguin magmas compared with those of Deception and Bridgeman Islands. The trend shown by the Penguin Island clinopyroxenes is unusual in that there is a marked initial enrichment in Ca (together with Al, Ti and Na) with increasing Fe/Mg ratio (Fig. 5). Although limited in extent, the trend appears to continue at constant Ca content corresponding to the crystallization of salitic pyroxenes. Moderate to high-Al salites are characteristic of alkaline suites but also occur in some calc-alkaline rocks. The Penguin Island pyroxenes are very similar to those described from Soufrière, St. Vincent, by Lewis (1973a and b).

4.3. Plagioclase Feldspars

(a) Deception Island. Plagioclase phenocryst compositions in the range An_{83-66} have been determined in an Mg-rich Deception Island basalt (B138.2). Thin sodic rims on these phenocrysts are of composition $An_{44}\ Or_3$ and correspond to the composition of the groundmass crystals. Phenocrysts in a typical andesite (B184.2) have the compositional range An_{42-35} with Or 1–2 wt%. Those in the dacites are An_{28-19} with 2% Or. Optical determinations suggest that there is a continuous chemical series in the Deception Island feldspars from An_{85} to about An_{15}. Slightly more calcic plagioclase (An_{88}) has been reported by Baker et al. (1975) in gabbroic cumulate blocks.

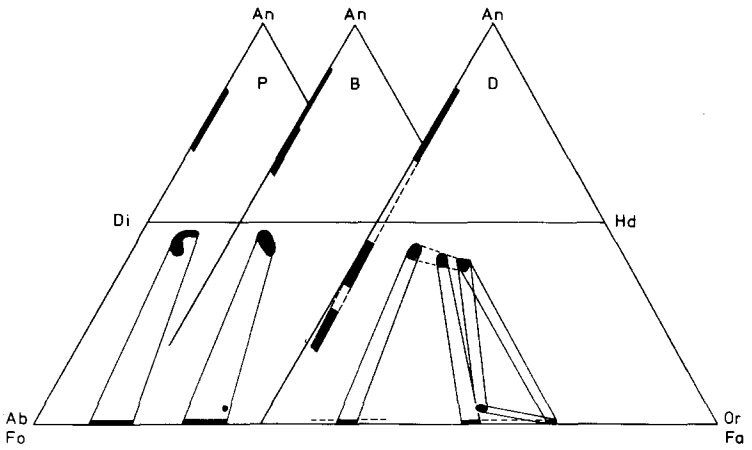

Fig. 5. Electron microprobe phenocryst data for Penguin, Bridgeman and Deception lavas plotted on composite feldspar-pyroxene-olivine ternary diagrams. Compositional fields are indicated in black; solid lines are tie lines; dashed lines indicate compositional trends

(b) Bridgeman Island. The total range of plagioclase phenocryst compositions measured in the single basalt specimen investigated using the microprobe is An_{89-64}. In the more sodic compositions, Or reaches 2%.

(c) Penguin Island. The total range of plagioclase compositions measured is An_{84-68}. Most crystals are normally zoned having calcic cores progressing to more sodic rims. Up to 1 wt% iron oxide is present in the feldspars and the Or content is always less than 1%.

4.4 Oxide Minerals

(a) Deception Island. Microphenocrysts of magnetite and ilmenite coexist in Deception Island basalts. Andesites contain a single titanomagnetite phase whereas dacites have microphenocrysts of ilmenite containing lamellae of titanomagnetite.

(b) Penguin Island. Small microphenocrysts of chromite are present as intergranular crystals or as inclusions in olivine phenocrysts in the more Mg-rich varieties of Penguin Island basalt. These minerals are magnesiochromites and ferroan chrome-spinels and range in composition as follows: Cr_2O_3 49.3–29.2%, total FeO 20.2–31.9% and MgO 12.5–14.7%.

5. Geochemistry

A total of 50 samples from Deception Island has been analysed. Of these 30 were collected in 1957–58 by D.D. Hawkes and are described in Hawkes (1961). A further 14 were collected by P.E. Baker and co-workers in 1968–70 and are described in Baker et al. (1975). The remainder were collected by ADS and SDW during a brief landing on the island in 1975. A total of 24 samples from Bridgeman Island and 21 samples from Penguin Island, collected in 1975 by ADS and SDW, has been analysed.

5.1. Analytical Methods

Samples were analysed for major and trace elements using the University of Birmingham, Philips PW1450 automatic X-ray fluorescence spectrometer. All elements were determined on 46 mm pressed powder pellets using Cr, W, and Mo tubes. Calibrations were based on international and laboratory standard rocks and spiked rock powders. Trace element results were corrected for mass absorption effects using WL_β and MoK_α Compton scatter lines. The rare-earth element analyses were determined by mass spectrometric isotope dilution using methods similar to those described by Hooker et al. (1975). Strontium isotopes were measured using methods described by Pankhurst and O'Nions (1973). Values for FeO, CO_2, and H_2O have not been determined, but representative analyses covering the range of rock types studied can be found in Gonzalez-Ferran and Katsui (1970) and Baker et al. (1975).

A simple arbitrary classification of the subalkaline volcanic rocks of Bransfield Strait, based on silica content, is used in this paper, as follows: basalt (< 53%), basaltic andesite (53–56%), andesite (56–62%), dacite (62–68%) and rhyodacite (68–72%).

5.2. Major Element Chemistry

Chemical analyses of representative lavas from the three volcanoes of Bransfield Strait are given in Tables 1 and 2. The lavas of Deception and Bridgeman Islands are subalkaline according to the definition of Irvine and Barager (1971) whereas compositions of Penguin Island basalts fall across the division between the alkaline and subalkaline groups (Fig. 6). Basaltic rocks of Deception and Bridgeman plot within, or close to, Kuno's (1966) high-alumina basalt (calc-alkaline) series.

On the $A(Na_2O+K_2O)$ – $F(FeO_T)$ – M(MgO) diagram (Fig. 7), the trend of the Deception Island compositions is one of moderate Fe-enrichment lying close to the line proposed by Irvine and Barager (1971) which divides calc-alkaline from tholeiitic rocks. The Bransfield Strait lavas do not exhibit the pronounced Fe-enrichment trends characteristic of abyssal tholeiites and island arc tholeiites (Ringwood, 1974).

The Deception suite forms a compositional series from basalt to rhyodacite but only basalts and basaltic andesites occur on Bridgeman and Penguin Islands.

Table 1. Representative analyses of Deception Island lavas

	1	2	3	4	5	6	7	8	9	10	11	12
Sample No.	B.138.2	B.103.3	B.213.2	B.119.1	B.311.1	B.202.1	B.428.1	B.184.1	B.107.8	B.111.3	P.870.1	B.317.1
SiO_2	51.89	52.33	52.71	52.46	54.60	54.79	57.50	61.91	62.57	67.39	68.02	70.10
TiO_2	1.49	1.56	1.68	2.44	2.46	2.10	2.16	1.26	1.21	0.63	0.55	0.50
Al_2O_3	16.20	16.64	16.12	15.12	14.27	16.00	14.83	15.32	15.26	14.73	14.99	14.31
Fe_2O_3[a]	9.46	9.33	9.96	12.16	11.81	9.06	8.66	7.25	7.17	5.27	4.97	4.32
MnO	0.18	0.17	0.18	0.21	0.21	0.21	0.21	0.21	0.22	0.19	0.18	0.13
MgO	6.11	5.19	4.92	4.08	3.89	4.05	3.19	1.35	1.24	0.49	0.33	0.90
CaO	10.07	9.97	9.09	8.37	6.92	7.24	5.94	3.57	3.63	1.87	1.69	3.46
Na_2O	4.07	4.57	4.90	5.09	5.08	5.38	5.71	6.70	6.44	7.35	7.45	4.88
K_2O	0.28	0.40	0.45	0.48	0.60	0.66	0.78	1.21	1.21	1.58	1.69	0.65
P_2O_5	0.21	0.26	0.29	0.33	0.30	0.27	0.29	0.41	0.30	0.11	0.10	0.08
Total	99.96	100.42	100.30	100.74	100.14	99.76	99.27	99.19	99.23	99.61	99.97	99.33
qz[b]	–	–	–	1.9	2.4	0.5	5.4	8.8	10.7	13.4	13.5	29.6
or	1.7	2.4	2.7	2.8	3.6	3.9	4.7	7.2	7.2	9.4	10.0	3.9
ab	34.6	38.7	41.6	43.0	43.3	45.9	48.9	57.4	55.1	62.6	63.2	41.7
an	25.3	23.8	20.7	17.0	14.4	17.7	12.7	8.3	9.3	2.6	2.5	15.4
di	19.3	19.8	18.6	17.7	15.1	13.8	12.6	6.0	6.0	5.3	4.7	1.2
hy	7.9	1.4	1.9	3.6	12.1	10.7	7.5	6.0	5.8	3.1	2.8	5.4
ol	4.9	7.5	7.4	–	–	–	–	–	–	–	–	–
mt	3.0	2.9	3.1	3.8	3.7	2.8	3.4	2.8	2.8	2.0	1.9	1.7
il	2.8	3.0	3.2	4.6	4.7	4.0	4.1	2.4	2.3	1.2	1.0	1.0
ap	0.5	0.6	0.7	0.8	0.7	0.6	0.7	1.0	0.7	0.3	0.2	0.2
Cr	141	101	52	20	28	20	13	9	9	6	7	20
Ni	35	19	15	9	10	7	4	3	4	3	2	6
Rb	3.0	5.0	5.2	5.6	9.2	10	13	20	21	31	32	14
Ba	88	102	99	89	138	133	161	199	205	230	242	68
Sr	340	427	383	357	380	369	337	255	260	141	134	117
La	8	8	10	12	12	15	21	25	28	30	28	10
Ce	21	24	29	31	33	39	40	61	61	68	64	22
Y	26	27	33	38	39	43	45	66	66	72	71	36
Zr	144	172	190	214	252	270	325	457	496	632	665	178
Nb	2	3	7	6	6	7	11	13	14	14	17	3
Pb	4	5	2	5	5	5	8	12	8	12	12	9
Th	2	3	1	1	1	1	4	4	4	7	7	2
Ga	16	20	22	24	24	24	20	24	25	26	27	6
Zn	76	73	80	87	100	96	103	123	123	134	124	101

[a] Total iron oxide as Fe_2O_3

[b] For CIPW norm, $Fe_2O_3/FeO = 0.3$ for lavas with $< 55\%$ SiO_2, $Fe_2O_3/FeO = 0.4$ for lavas with $> 55\%$ SiO_2

Key: 1 = B.138.2, Deception basalt, plag (3), oliv (2), oliv (2), cpyx (1). 2 = B.103.3, Deception basalt, plag (2), oliv (1). 3 = B.213.2, Deception basalt, aphyric. 4 = B.119.1, Deception basalt. 5 = B.311.1, Deception basaltic andesite. 6 = B.202.1, Deception basaltic andesite, plag (3), cpyx (1). 7 = B.428.1, Deception andesite. 8 = B.184.1, Deception andesite, plag (10), cpyx (2), oliv (1), ore. 9 = B.107.8, Deception dacite, plag (7), cpyx (1), oliv (1), ore. 10 = B.111.3, Deception dacite, plag (12), oliv (2), cpyx (1), opyx (1), ore (1). 11 = P.870.1, Deception rhyodacite, plag (10), cpyx (1), oliv (1), opyx (1), ore (1). 12 = B.317.1, Deception rhyodacite, aphyric

Note: Figures in brackets indicate phenocryst modal percentages

The normative characteristics of the lava groups are illustrated in the Ne-Di-Ol-Qz diagram (Fig. 8). Basalts from Deception and Penguin plot close to the Di-Ol join. Penguin basalts are slightly undersaturated containing up to 4% *ne* whereas Deception basalts are olivine- and quartz-tholeiites. All of the Bridgeman lavas are quartz-tholeiites. Compared with the alkaline, calc-alkaline and tholeiitic suites of the Lesser Antilles island arc (Brown et al., 1977), the Bransfield Strait lavas contain significantly lower proportions of normative olivine (Fig. 8) and have higher Di/Ol ratios. The Bransfield Strait lavas are less aluminous than the Lesser Antilles suites so that the former contain less normative anorthite and consequently more normative diopside than equivalent rocks from the Caribbean. Compositions of some abyssal basalts plotted on the Di-Ol-Qz diagram (Fig. 8) are similar to the quartz-tholeiites from De-

Table 2. Representative analyses of Penguin Island and Bridgeman Island lavas

Sample No.	1 P.721.3	2 P.802.1	3 P.808.1	4 P.807.2	5 P.810.4	6 P.640.1b	7 P.642.4	8 P.642.2c	9 P.640.3a	10 P.646.1
SiO_2	49.02	49.25	49.30	49.57	49.28	52.88	53.04	54.72	54.06	53.96
TiO_2	1.08	1.22	1.22	1.19	1.26	0.64	0.58	0.60	0.75	0.64
Al_2O_3	15.81	15.34	16.58	16.64	17.23	17.68	18.26	18.83	19.04	18.17
Fe_2O_3[a]	9.95	10.39	9.62	9.54	9.81	7.43	7.39	6.87	7.51	7.38
MnO	0.18	0.18	0.18	0.17	0.18	0.13	0.13	0.13	0.13	0.13
MgO	8.95	8.84	7.74	7.79	6.78	6.14	5.94	5.04	4.39	5.10
CaO	10.08	10.46	10.03	10.15	9.71	10.30	10.37	9.85	9.33	9.50
Na_2O	3.95	3.70	4.13	4.18	4.30	3.54	3.11	3.49	3.86	3.61
K_2O	0.48	0.47	0.58	0.60	0.60	0.47	0.53	0.57	0.57	0.67
P_2O_5	0.28	0.26	0.32	0.42	0.30	0.06	0.06	0.07	0.06	0.07
Total	99.78	100.11	99.70	100.25	99.45	99.27	99.41	100.17	99.70	99.23
qz	–	–	–	–	–	0.2	2.1	3.7	2.4	2.5
ne[b]	3.5	2.2	3.6	3.7	3.7	–	–	–	–	–
or	2.9	2.8	3.5	3.6	3.6	2.8	3.2	3.4	3.4	4.0
ab	27.2	27.4	28.6	28.7	30.0	30.3	26.6	29.6	32.9	30.9
an	24.2	24.0	25.2	24.9	26.2	31.3	34.7	34.1	33.2	31.8
di	19.8	21.5	18.7	18.6	16.9	16.3	13.8	11.8	10.8	12.7
hy	–	–	–	–	–	15.3	16.0	13.9	13.3	14.3
ol	16.5	15.8	14.3	14.2	13.3	–	–	–	–	–
mt	3.1	3.2	3.0	3.0	3.1	2.3	2.3	2.1	2.3	2.3
il	2.1	2.3	2.3	2.3	2.4	1.2	1.1	1.1	1.4	1.2
ap	0.7	0.6	0.8	1.0	0.7	0.1	0.1	0.2	0.1	0.2
Cr	494	447	307	306	192	130	87	67	40	59
Ni	159	137	107	107	78	40	28	22	20	30
Rb	5.2	5.7	4.9	5.7	7.3	11	12	11	14	18
Ba	148	132	146	157	173	70	86	80	84	101
Sr	534	536	612	615	657	332	311	319	346	283
La	10	7	9	10	12	2	4	3	2	3
Ce	20	19	22	24	23	10	8	8	9	8
Y	12	10	11	13	10	10	11	9	11	13
Zr	80	80	85	89	92	58	69	76	76	86
Nb	2	4	4	4	4	1	1	1	1	1
Pb	7	6	7	6	10	5	5	4	7	6
Th	1	1	1	1	1	2	1	1	1	4
Ga	21	22	25	29	26	19	19	21	22	20
Zn	69	78	73	76	77	62	62	64	65	67

[a] Total iron oxide, as Fe_2O_3

[b] For CIPW norm, $Fe_2O_3/FeO = 0.2$ for Penguin lavas and $Fe_2O_3/FeO = 0.3$ for Bridgeman lavas

Key: 1 = P.721.3, Penguin basalt, oliv (15), cpyx (5). 2 = P.802.1, Penguin basalt, oliv (12), cpyx (5). 3 = P.808.1, Penguin basalt, cpyx (10), oliv (5). 4 = P.807.2, Penguin basalt, oliv (7), cpyx (5), plag (3). 5 = P.810.4, Penguin basalt, cpyx (10), oliv (7), plag (5). 6 = P.640.1b, Bridgeman basalt, plag (20), oliv (7), cpyx (1). 7 = P.642.4, Bridgeman basaltic andesite, plag (25), cpyx (5), oliv (3). 8 = P.642.2c, Bridgeman basaltic andesite, plag (25), cpyx (10), oliv (2). 9 = P.640.3a, Bridgeman basaltic andesite, plag (30), cpyx (5), oliv (2). 10 = P.646.1, Bridgeman basaltic andesite, plag (25), cpyx (7), oliv (2)

Note: Figures in brackets indicate phenocryst modal percentages

ception and Bridgeman Islands but of course the latter are considerably more feldspathic than ocean-floor basalts.

One of the main characteristics of the Bransfield Strait lavas, illustrated in the K_2O–SiO_2 plot (Fig. 9) is their low-K nature. On this diagram, the Bridgeman samples fall on the pronounced linear trend produced by the Deception rocks. The Deception trend coincides with those for the calc-alkaline rocks of Dominica (Brown et al., 1977) and the high-K_2O lavas of the South Sandwich Islands (Thule, Cook, Leskov and Visokoi) (Baker, 1978). Penguin basalts have higher K_2O/SiO_2 ratios than those from Deception and Bridgeman. Extrapolation of the Deception trend to slightly lower SiO_2 levels leads into a field occupied by abyssal basalts and island arc tholeiites from the

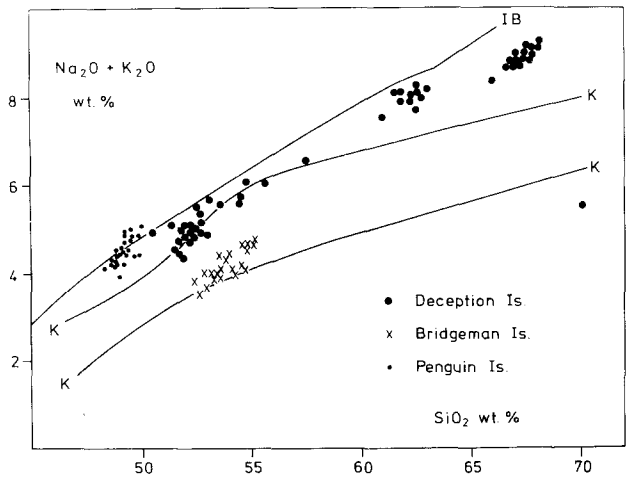

Fig. 6. Alkalis-silica plot for Bransfield Strait lavas. IB is the line dividing alkaline and subalkaline fields of Irvine and Baragar (1971). K's denote the field boundaries of the high-alumina basalt series of Kuno (1966)

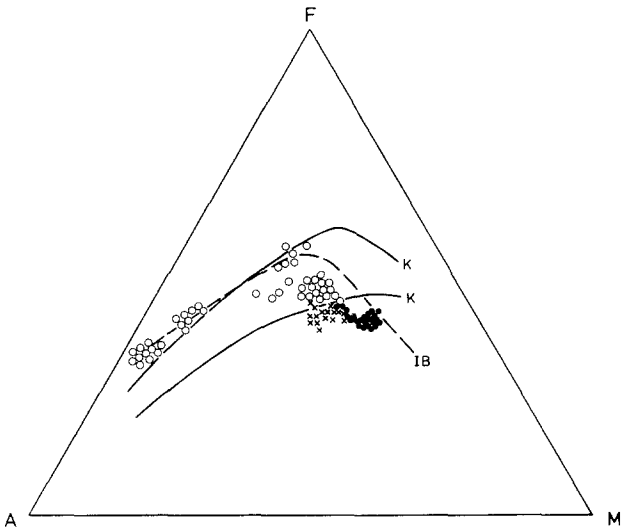

Fig. 7. $A(Na_2O+K_2O)$-F(FeOT)-M(MgO) diagram for Bransfield Strait lavas. IB divides tholeiitic and calc-alkaline fields of Irvine and Baragar (1971). K's denote the limits of Kuno's (1968) hypersthenic (calc-alkaline) series

Lesser Antilles and the South Sandwich Islands (Fig. 9).

Andesites and dacites of Deception Island are characterized by very high levels of Na_2O (Table 1); up to 7.5%, although the peralkaline condition is never achieved. Even the basalts from Deception are unusually sodic, with over 4% Na_2O. All of the Bransfield Strait lavas have high Na/K ratios, the ratios in basaltic rocks from Deception Island being matched only by those in ocean-floor basalts (Fig. 10). Bridgeman Island basalts and basaltic andesites are very similar to those from Deception Island,

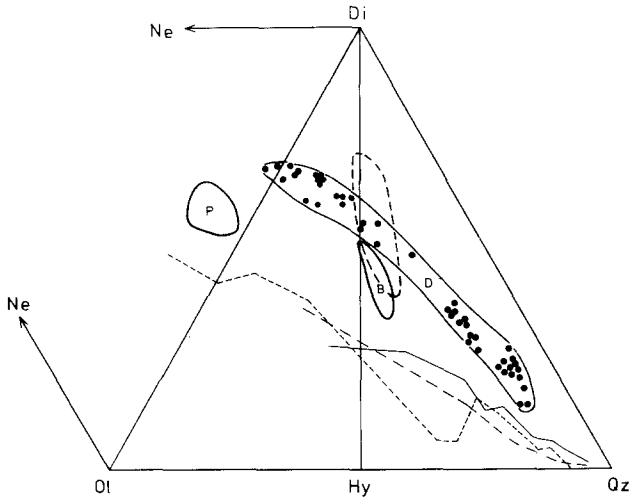

Fig. 8. Normative Di-Ol-Qz-Ne plot for Bransfield Strait lavas. Fields for Penguin, Bridgeman and Deception *(points plotted)* samples are indicated. The dashed field is that of DSDP Leg 34 basalts (Kempe, 1976). Lesser Antilles trends from Brown et al. (1977) are plotted as follows: *solid line:* St. Kitts (tholeiitic); *long dashed line:* Dominica (calc-alkaline); *short dashed line:* Grenada (calc-alkaline)

but have higher Al and Ca, consistent with a higher content of modal plagioclase. There are also some significant trace element differences.

5.3. Trace Elements

Trace element data on representative lavas from Deception, Penguin and Bridgeman Islands are presented in Tables 1 and 2. There are some systematic within-island variations, but also some significant differences between the basaltic rocks of the three islands. In general terms the concentrations of some incompatible elements (K, Rb, and Ba) are at the lower ends of the ranges observed in calc-alkaline suites and overlap those for island arc tholeiites and even mid-ocean ridge basalts, although Ba is significantly higher than in most ridge basalts. Variations within, and differences between, the three islands are best illustrated by plotting elements and oxides against an incompatible element (Fig. 11). Zirconium is chosen here because it is abundant and can be determined with high precision by XRF techniques. Although perhaps not the most incompatible trace element (Wood et al., in press) it does have a very low bulk distribution coefficient in basaltic systems (Weaver et al., 1972; Tarney et al., 1977; Saunders and Tarney, in press).

A feature of all the trace element plots is the smooth and extensive trends shown by the Deception Island lavas, whereas Penguin and especially Bridge-

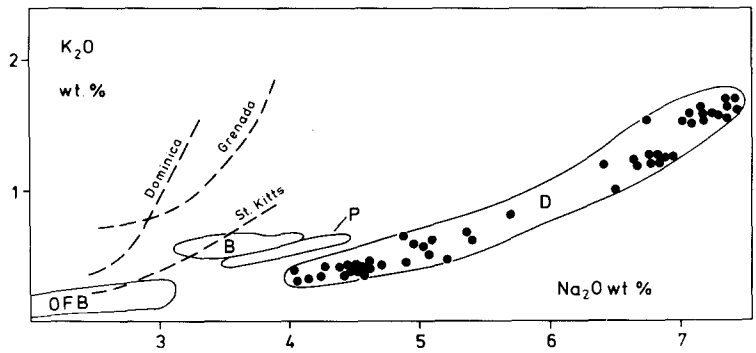

Fig. 9. K_2O-SiO_2 plot for Bransfield Strait lavas – fields indicated. Trends for Lesser Antilles volcanics after Brown et al. (1977) are shown as in Figure 8. *Dashed-dotted line* is the low-K_2O trend for the South Sandwich Islands (Baker, 1978)

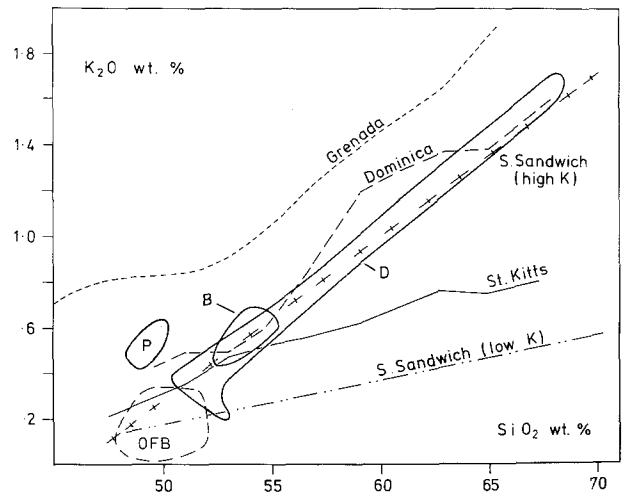

Fig. 10. K_2O-Na_2O plot for Bransfield Strait lavas. Trends for the Lesser Antilles suites (Brown et al., 1977) are indicated. The field *OFB* contains points for 150 ocean floor basalt analyses taken from the literature

man lavas show much more limited ranges. SiO_2 enrichment within the Deception suite is proportional to that of Zr, and Na_2O systematically increases until limited by separation of sodic plagiocalse in the more sodic magma compositions. The behaviour of Sr also reflects plagioclase separation in that there is a negative correlation with Zr, especially in the more sodic magmas where Sr enters more easily into sodic plagioclase. It is likely that Ba is also entering sodic plagioclases to a limited extent because, although Ba increases progressively throughout the compositional range, Ba/Zr ratios decrease. On the other hand K_2O and Rb increase colinearly with Zr showing that no potassic mineral phase was crystallising. A sympathetic relationship with Zr is exhibited by Nb, Ce and Y, although Ce/Zr and Y/Zr ratios tend to decrease at higher Zr and SiO_2 levels, suggesting that Ce and Y are partitioning increasingly into the major mineral phases as the magma with which they are in equilibrium becomes more silicic (as suggested by Watson, 1976). Apatite separation occurs in the intermediate magmas and is marked by a sharp fall in P_2O_5. However, Ce/Zr and Y/Zr ratios show only a slight inflexion at this point, indicating that, although the rare-earth elements partition strongly into apatite, the amount of apatite separating is too small to affect the overall levels of rare earth elements in the magma.

A plot of TiO_2 against Zr shows an initial enrichment up to about 2.5% TiO_2 at 200–350 ppm Zr. However, in the more evolved andesitic lavas TiO_2 rapidly decreases owing to separation of titanomagnetite. FeO shows a similar pattern of behaviour. It is interesting that it is at this point that SiO_2 begins to rise with increasing Zr, suggesting that titanomagnetite separation has triggered the trend towards siliceous magma compositions. A similar feature is seen in the Sarmiento marginal basin ophiolite complex in S. Chile (Saunders et al., 1979) where titanomagnetite separation from titanium- and iron-rich tholeiitic differentiates yielded plagiogranites rich in Zr and Y.

The moderately low contents of MgO (6%), Cr (114 ppm) and Ni (35 ppm) in the most basic Deception lavas suggests they are not primary mantle melts, but have undergone considerable pre-eruptive fractional crystallisation involving olivine and clinopyroxene and/or chrome spinel. The relatively high Zr contents of these lavas also suggests this, although the levels of Zr and other incompatible elements are more dependent on the degree of partial melting. MgO, Cr, and Ni rapidly become further depleted in the Deception suite, again probably because of pyroxene and olivine fractionation ($K_{D_{Ni}}^{Ol/L} > K_{D_{Ni}}^{Cpx/L} > K_{D_{Cr}}^{Cpx/L} \gg 1$; Leeman, 1976).

The very high Cr (500 ppm) and Ni (170 ppm) contents of the most magnesian Penguin Island basalts indicates that they are closer to primary mantle melts. Although the range of Zr abundances is much less then that of Deception lavas, significant fractionation has taken place, as demonstrated by the rapid fall in Cr and Ni values as Zr and the other incompatible elements increase. These systematic variations can be explained almost completely by fractional crystal-

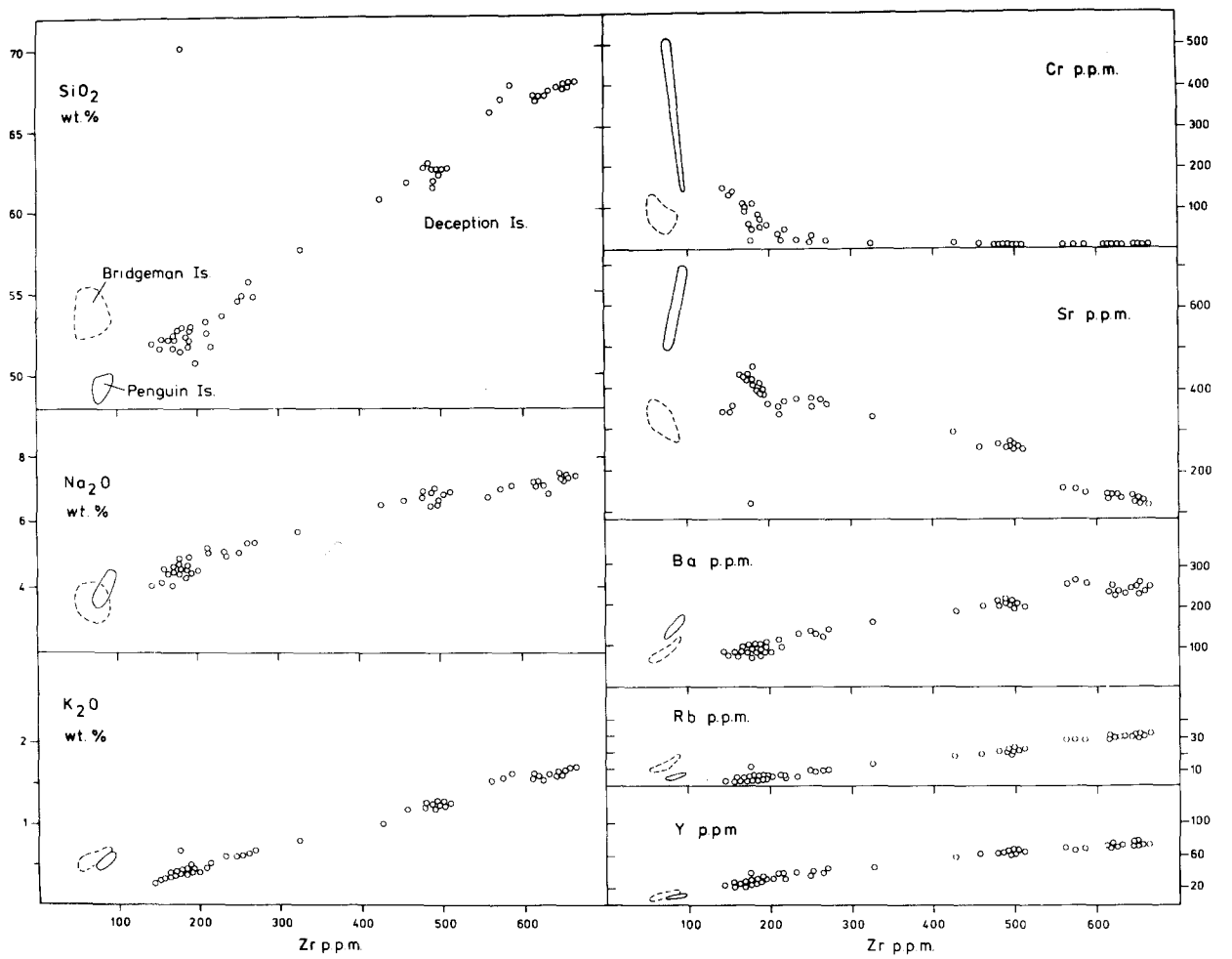

Fig. 11. Plots of selected major oxides and trace-elements against Zr. Fields for Penguin and Bridgeman Islands are shown and individual points are plotted for Deception Island

lisation of olivine, clinopyroxene and/or chromite. Thus Penguin basalts are characterised by steep, sharply defined colinear trends on Figure 11, and they generally have higher abundances of K, Rb, Ba, Sr, Ti, P, Na, Ni, and Cr at equivalent Zr levels than the Deception basalts. The high incompatible-element/Zr ratios are clearly a characteristic of the primary Penguin magmas. This could be accounted for by retention of some Zr in the mantle source by a mineral such as garnet, which would also be expected to retain Y and the heavy REE. Note that Y/Zr ratios are lower in Penguin basalts than in the lavas of Deception and Bridgeman Islands.

Penguin Island basalts show a marked increase in Sr with increasing Zr, and Sr is clearly behaving as an incompatible element. Of course plagioclase phenocrysts occur only in the most evolved Penguin basalts, whereas plagioclase was a fractionating phase in most of the Deception magmas and caused depletion of Sr. Note that the most primitive Deception basalts (i.e., those with the lowest Zr) have lower Sr than in the other basalts of the Deception suite, suggesting that Sr may have been acting incompatibly in Deception magmas too until plagioclase separation occurred.

Bridgeman Island lavas plot in tight clusters on the trace element versus Zr plots in Figure 11, contrasting with the strong trends shown by the Deception and Penguin lavas. An interesting feature is that, although they appear more evolved in terms of major elements (e.g., SiO_2, K_2O) than the Penguin and Deception basalts, they have distinctly lower absolute abundances of incompatible elements such as Ti, P, Sr, Zr, Nb, Y, Ce, and La, coupled with low values for Cr and Ni. This feature is typical of island arc tholeiite suites and also *some* back-arc basalts from the spreading centre in the East Scotia Sea (Saunders and Tarney, in press). Many of these elements when plotted against Zr lie on similar trends to the Deception lavas. However, Ba, and especially K and Rb

Table 3. Mass-spectrometric data on selected Bransfield Strait samples

Sample No.	Ba	Ce	Nd	Sm	Eu	Gd	Dy	Er	Yb	$^{87}Sr/^{86}Sr$
Penguin I.										
P.721.3	161	22.6	13.1	3.04	1.06	3.06	2.84	1.59	1.49	0.70387±6
P.808.1	–	–	–	–	–	–	–	–	–	0.70386±5
P.810.4	–	–	–	–	–	–	–	–	–	0.70386±5
P.807.2	178	26.6	15.6	3.51	1.25	3.45	3.18	1.79	1.65	0.70396±4
Bridgeman I.										
P.640.1b	77	7.92	5.47	1.56	0.65	1.90	2.02	1.25	1.15	0.70349±5
P.640.3a	–	–	–	–	–	–	–	–	–	0.70346±4
P.642.2c	79	9.27	6.12	1.75	0.61	2.16	2.28	1.48	1.33	0.70344±5
P.646.1	–	–	–	–	–	–	–	–	–	0.70359±4
										0.70356±5
Deception I.										
B.138.2	80	21.9	14.4	3.94	1.46	4.83	4.92	3.21	2.99	0.70336±4
B.103.4	76	23.7	16.1	4.21	1.48	4.76	5.04	3.06	2.74	–
B.103.3	79	24.1	16.3	4.26	1.50	4.88	5.05	3.06	2.78	0.70346±5
B.202.1	126	39.6	22.5	5.51	1.81	6.29	6.48	4.10	3.84	0.70342±5
B.107.8	200	61.5	34.7	8.64	2.36	9.16	9.74	6.43	6.12	0.70347±5
P.870.1	251	70.6	33.6	8.02	1.75	8.44	9.32	6.22	6.20	0.70342±4

Concentrations in ppm, ±2% for most rare earth elements, ±5% for Ba
$^{87}Sr/^{86}Sr$ ratios normalised to 0.70800 for Eimer and Amend standard, errors are 2 S.E.M.

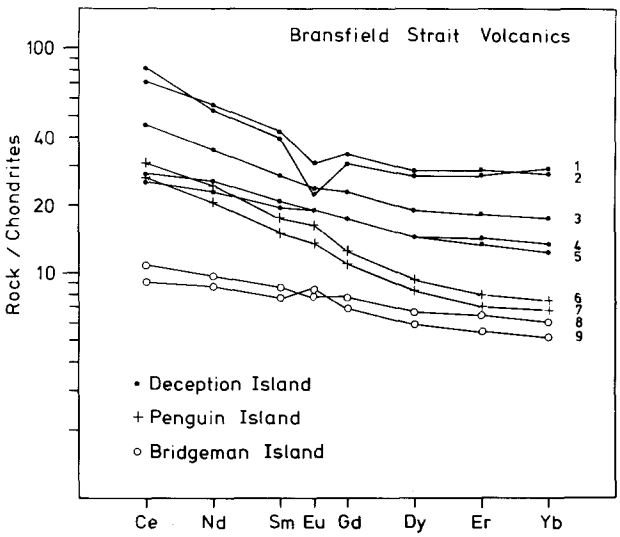

Fig. 12. Mass-spectrographic REE data of Table 3 displayed on a chondrite-normalised plot. Numbered patterns are as follows: 1-P.870.1, 2-B.107.8, 3-B.202.1, 4-B.138.2, 5-B.103.3 and B.103.4, 6-P.807.2, 7-P.721.3, 8-P.642.2c, 9-P.640.1b

are notable exceptions and are enriched in Bridgeman lavas, which have markedly higher K/Zr, Rb/Zr and Ba/Zr ratios (Table 4) than equivalent basaltic andesites on Deception.

It is interesting in comparing these three volcanoes, to note not only the decoupling of trace element behaviour from that of the major elements, and of K, Rb and Ba from the other incompatible elements, but also Ba from K and Rb. Thus Ba/Zr ratios are higher in Penguin basalts than in Bridgeman and Deception lavas (Fig. 11, Table 4) but Bridgeman has the highest K/Zr and especially Rb/Zr ratios. K/Ba ratios of Penguin lavas are lower than those of Deception and much lower than those of Bridgeman. K/Rb ratios in Deception and Penguin basalts are high, and approach those in typical "depleted" MORB. Rb/Sr ratios are likewise very low and analogous to the ratios in MORB. With regard to K/Ba and K/Sr ratios however, it is the Bridgeman lavas which have the higher MORB-like values, whereas Rb/Sr ratios of Bridgeman lavas are high and comparable to those of island arc and calc-alkaline basalts.

These decoupled relationships contrast with the much more coherent behaviour of incompatible trace elments in North Atlantic Ridge basalts (Tarney et al., in press; Wood et al., in press). Thus criteria which are normally used to indicate "enriched" and "depleted" geochemical characteristics are here conflicting. Zr/Nb ratios are high in all the Bransfield Strait lavas (even the alkalic Penguin basalts) and are comparable with those in the most depleted MORB samples (Erlank and Kable, 1976). Yet Ce_N/Y_N ratios, Ba and Sr are markedly higher than in MORB and more typical of transitional basalts from Iceland and the Reykjanes Ridge and MAR 45° N (Tarney et al., in press).

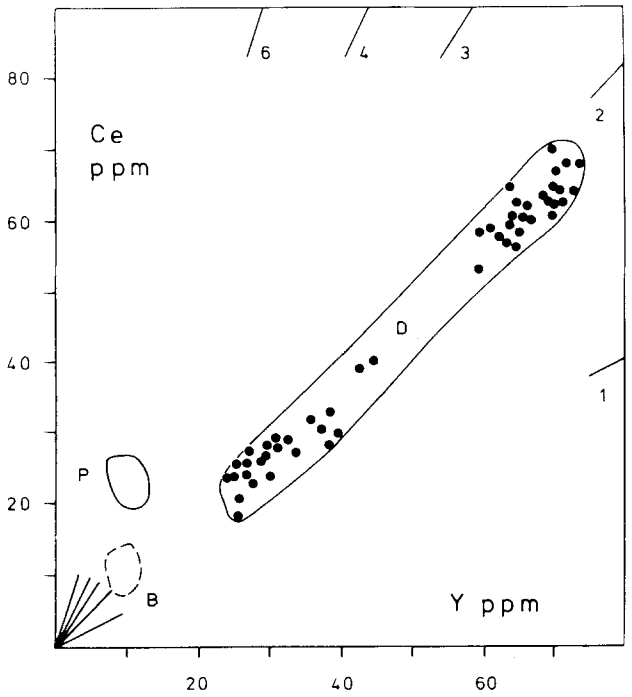

Fig. 13. X-ray fluorescence Ce-Y data for Bransfield Strait lavas. Chondritenormalized Ce/Y ratios are indicated

5.4. Rare Earth Elements

Rare earth element data for 6 Deception samples, 2 Bridgeman samples and 2 Penguin samples are given in Table 3 and the chondrite-normalised REE patterns are shown in Fig. 12. These samples were chosen as representative of the range of lava compositions from the three volcanoes. To confirm that this is so, a Ce versus Y plot (XRF data) for all the samples is shown in Fig. 13. Both plots demonstrate apparently simple rare earth characteristics. Bridgeman lavas have the lowest REE abundances (less than 10 times chondrites) and Ce_N/Yb_N ratios of 1.8. The most magnesian Deception lavas have similar Ce_N/Yb_N ratios but much higher REE abundances (ca. 20 times chondrites). Penguin Island basalts have similar heavy REE abundances to Bridgeman lavas whereas their light REE abundances are the same as in the more primitive Deception lavas; Ce_N/Yb_N ratios are much higher at 4.0, reflecting the more alkaline characteristics of the lavas. Basalts from all three volcanoes show small positive Eu anomalies, most marked in sample P.640.1b from Bridgeman Island.

Crystal fractionation processes within the Deception volcano have given rise to successively higher REE levels in the more silicic magmas, but there is only slight change in Ce/Yb ratio. That Y does not precisely behave like Yb but acts rather more like an intermediate REE is indicated by the smaller systematic increase in Ce_N/Y_N (1.7 to 2.0) compared with Ce_N/Yb_N (1.9 to 2.9). The dacites and rhyodacites have prominent negative Eu anomalies and more "concave-upwards" rare-earth patterns. The similarity between the rare-earth patterns of the Bridgeman and Deception lavas and those from the Sarmiento marginal basin ophiolite complex in S. Chile (Saunders et al., 1979) is striking.

5.5. Strontium Isotopes

High precision $^{87}Sr/^{86}Sr$ ratios for 13 Bransfield Strait lavas are listed in Table 3. There is a clear distinction between Penguin Island (average 0.70389) and the other two islands, most of the samples from which overlap in the range 0.70340 to 0.70350. This range is extended well beyond analytical error by values of 0.70336 ± 4 for the most magnesian Deception Island basalt and 0.70358 ± 4 for one of the Bridgeman Island samples.

Table 4. Trace-element ratios for selected Bransfield Strait lavas

	Penguin I.		Bridgeman I.		Deception I.				
Sample No.	P.721.3	P.807.2	P.640.1b	P.642.2c	B.138.2	B.103.3	B.202.1	B.107.8	P.870.1
K/Rb	770	870	350	430	770	660	550	480	440
K/Ba	25	28	51	60	29	42	43	50	56
K/Sr	7.7	7.9	12	15	6.8	7.9	15	39	110
Rb/Sr	0.010	0.009	0.033	0.034	0.009	0.012	0.027	0.081	0.24
Sr/Ba	3.3	3.5	4.3	4.0	4.3	5.4	2.9	1.3	0.5
Ce_N/Sm_N	1.7	1.8	1.2	1.2	1.3	1.3	1.7	1.7	2.1
Ce_N/Yb_N	3.9	4.1	1.8	1.8	1.9	2.2	2.6	2.6	2.9
Ce_N/Y_N	3.9	4.2	1.6	2.1	1.7	1.8	1.9	1.9	2.0
Eu/Eu*	1.06	1.09	1.16	0.96	1.03	1.01	0.94	0.81	0.65
Zr/Nb	47	23	58	76	85	54	36	35	39

6. Petrogenesis

Discussion of the genetic relationships between the various volcanic rocks of Bransfield Strait depends largely on the interpretation of the trace element and isotopic data. Of particular significance are the differences in the concentrations of elements and the values of certain trace element ratios. In principle the observed variations may result from any of three major causes or combinations thereof: compositional and/or mineralogical differences in the source material, differing degrees of partial melting under different P, T, P_{H_2O}, f_{O_2} conditions, and modifications of the primary magma chemistry by processes dominated by crystal fractionation.

Closed-system crystal fractionation has little effect on incompatible trace element ratios until extreme degrees of solidification are reached. O'Hara (1977) has devised an open-system process which can account for rather more variation in the trace element chemistry of co-magmatic lavas, but this mechanism is by no means as effective as differential partial melting for producing large changes in, for example, Ce/Sm and Ce/Yb ratios (Pankhurst, 1977). High-level crystal fractionation may account for much of the within-island variation, and this process appears to have been primarily responsible for the production of large volumes of intermediate and silicic magma on Deception. However, we believe that the incompatible element ratios of the *basalts* of the three Bransfield Strait volcanoes, listed in Table 4, may be used to assess source material compositions and the nature of the melting events.

6.1. Penguin Island

Of all the Bransfield Strait lavas, the olivine-basalts of Penguin Island have the most primitive chemistry (low SiO_2, high MgO) and are therefore likely to represent the least modified mantle melts. The lack of significant crystal fractionation is reflected in moderately high concentrations of Ni (up to 170 ppm), Cr (up to 510 ppm) and Sr (530–690 ppm). The absence of plagioclase phenocrysts from Mg-rich Penguin basalts indicates that this mineral was not on the liquidi for these compositions and is therefore unlikely to have been present in the source material, a suggestion which is confirmed by the lack of large positive Eu anomalies in the Penguin basalt REE patterns. As plagioclase-free mantle is unlikely to have a Sr content in excess of 50 ppm relatively small degrees of partial melting ($< 10\%$) are indicated. High Ce/Sm, Ce/Yb and Ce/Y ratios also suggest small degrees of melting with heavy-REE and Y being retained in garnet in the refractory residue. In this respect Penguin Island basalts resemble the mildly alkaline basalts of the Eastern Neovolcanic Zone in Iceland (Jakobsson, 1972; O'Nions et al., 1973).

A distinctive feature of their chemistry is the low content of large-ion alkali metals, K and especially Rb. Moreover, the Rb/Sr ratios of the Penguin basalts (ca. 0.01) are much too low to account for their observed $^{87}Sr/^{86}Sr$ ratios, i.e., they plot to the left of a 4,600 Ma isochron drawn through the composition of primordial Sr, as do typical abyssal tholeiites. For the latter rocks, two alternative hypotheses have been proposed to account for very low lithophile element contents: either that these elements were depleted in the source region as a result of previous melt extraction (Gast, 1968) or that they are retained during partial melting in a refractory phase such as phlogopite (Flower et al., 1975).

In order to elucidate the petrogenesis of the Bransfield Strait volcanics, and in particular, to test the above hypotheses, we have evaluated semi-quantitative melting models relating trace element concentrations in the source to those in extracted basaltic liquids based on partition coefficients compiled by Leeman (1976) and Hanson (1977). The problem is a complex one in that both the starting composition (mineralogical and chemical) and the degree of melting are unknown so that an infinite variety of solutions are calculable. We have restricted our models by making the reasonable, though not necessarily correct, assumption that chondrite-normalised REE patterns in the mantle should be essentially flat. Various degrees of melting of model mantle with possible mineralogical compositions were considered, using the same approach as Leeman (1976). The predicted enrichment factors were applied to the analytical data for primitive Bransfield Strait basalts in order to derive an *inferred* trace element composition for possible source regions. Representative solutions are shown in Table 5.

Example A investigates the refractory phlogopite model for Penguin basalt P.721.3 (it is generally supposed that other possible hydrous phases in the mantle, such as amphibole, would retain K but not Rb). It shows that such a magma could be derived from a source with a more "normal" Rb/Sr ratio of 0.03 only if phlogopite were present at about 5% in the mode and the degree of melting was as low as 3%. There is, however, an inherent contradiction in that the inferred K, Rb, and Ba concentrations of the source are at least five times too low for a peridotite with 5% phlogopite. Increasing the proportion of phlogopite or decreasing the degree of melting makes this problem worse, whereas altering them in the opposite sense makes it very difficult to retain significant

Table 5. Inferred source chemistry for selected melting models

	Penguin Island (P.721.3)			Bridgeman Island (P.640.1b)			Deception Is. (B.138.2)	
Model	A	B	C	D	E	F	G	H
Source mineralogy	Gnt-Phlog peridotite	Garnet peridotite	Garnet peridotite	Spinel peridotite	Spinel peridotite	Spinel peridotite	Spinel peridotite	Spinel peridotite
% Melt	3	3	10	10	15	20	5	10
Ce_N	1.4	1.3	3.1	0.9	1.3	1.6	1.5	2.4
Sm_N	1.4	1.4	2.2	0.9	1.2	1.4	1.7	2.3
Yb_N	1.9	1.7	1.6	0.7	0.8	1.0	1.3	1.7
K	540	129	401	316	471	627	95	188
Rb	0.7	0.2	0.5	0.9	1.3	1.8	0.1	0.2
Sr	26	24	60	30	43	56	18	31
Ba	6	5	16	6	9	12	3	6
Zr	5	5	11	6	8	11	7	14
Ce_N/Yb_N	0.7	0.8	1.9	1.3	1.5	1.6	1.2	1.4
Ce_N/Sm_N	1.0	0.9	1.4	1.0	1.1	1.1	0.9	1.1
Rb/Sr	0.03	0.006	0.008	0.03	0.03	0.03	0.007	0.008
K/Rb	771	819	799	355	355	354	781	777
K/Ba	90	25	25	50	50	50	29	29
K/Zr	108	26	36	53	59	57	14	27

REE concentrations are chondrite-normalised, remainder all ppm Bold type indicates the most favoured models. Partition coefficients were taken from the compilation of Hanson (1977) supplemented from Leeman (1976) where necessary. Zr was assumed to be incompatible ($D<0.01$) for all minerals except garnet, where a $D_{Zr}^{Gnt/L}$ of 0.6 was used. Batch melting equations were used for the computation

Source mineralogy (modal %) was as follows, with relative melting rates in parentheses: *A*=Olivine 50 (5), Opx 20 (10), Cpx 20 (20), Garnet 5 (15), Phlogopite 5 (50); *B* and *C*=Olivine 55 (10), Opx 20 (20), Cpx 20 (40), Garnet 5 (30); *D*–*H*=Olivine 51 (10), Opx 21 (20), Cpx 23 (60), Spinel 5 (10)

20% fractional crystallization of olivine and pyroxene from the Bridgeman and Deception Island primary melts has been accommodated in the modelling (see text)

phlogopite in the residue after melting. On this basis we feel that this model can be excluded.

Examples B and C for phlogopite-free garnet-peridotite show the effects of varying the degree of melting, those around 10% requiring a significantly light-enriched REE pattern in the source. We favour the smaller degree of melting illustrated in example B which predicts low K and Rb contents but reasonable REE, Sr, and Ba abundances in the source. It is interesting to note that ca. 20% melting of the same type of source would yield the trace element contents of a "hot-spot" or "fertile" basalt (light-enriched REE about 10 times chondrite, ca. 0.1% K, 1 ppm Rb, 150 ppm Sr, and 25 ppm Ba). The only further difficulty encountered in explaining the Penguin Island basalts is their relatively high $^{87}Sr/^{86}Sr$ ratios compared with oceanic tholeiites. In fact the values of ca. 0.7039 reported here are close to those of island arc tholeiites from the South Sandwich Islands where contamination with radiogenic Sr derived from the subducted lithosphere is suggested (Hawkesworth et al., 1977).

Finally, modelling was attempted to test whether the chemical variation within the Penguin Island basalts could be explained by crystal fractionation of the observed phenocryst phases. Results confirm that the major element differences between basalts P.721.3 (most Mg-rich) and P.810.4 (least Mg-rich) could be accounted for by about 12% solidification comprising 4.6% olivine (Fo_{82}), 6.0% clinopyroxene ($Ca_{44}Mg_{46}Fe_{10}$) and 1.4% plagioclase (An_{71}). The enrichments of incompatible elements such as Ba, Ce, and Zr suggest a concordant figure of about 14% solidification. The bulk distribution coefficients predicted by 14% Rayleigh type fractional crystallization are 6.1 for Ni and 7.8 for Cr, suggesting that clinopyroxene and possibly chrome-spinel form a major proportion of the crystallizing phases ($K_{D_{Ni}}^{Cpx/L}$ at 1200° C is 4.9, and $K_{D_{Cr}}^{Cpx/L}$ at 1200° C is 7.1; Leeman, 1973), with minor olivine fractionation ($K_{D_{Ni}}^{Ol/L}$ is 13 at 9% MgO, and 17 at 6.8% MgO; Hart and Davis, 1978). The significant fall in Ni and Cr contents rules out the possibility of chemical variation within Penguin Island basalts being due solely to differing degrees of partial melting.

6.2. *Bridgeman Island*

The basaltic lavas of Bridgeman Island are distinguished from those of the other two islands by their low Ba, Zr, Nb, P, light REE and K/Rb and their high Rb, Rb/Sr and K/Ba. Their REE patterns are essentially flat and have less than 10 times chondritic abundance. Thus they appear to be rather exten-

sive partial melts with a garnet-free residuum. A suitable melting model would involve 10–20% melting of spinel-peridotite, but the initial presence of small amounts of garnet, amphibole or plagiocalse cannot be excluded since these would all be consumed after a relatively small degree of melting. Another major difficulty is the low Cr and Ni content of any solid residue with which the basalt would be in equilibrium. The Ni content is a factor of about 10 too low for a truly "primary" mantle melt, presumably reflecting its removal in crystallised cumulates. This can be accounted for, with very considerable uncertainty, by about 20% removal of olivine, pyroxenes and Cr-spinel (assuming $D_{Ni} \sim 10$; Leeman, 1973; Hart and Davis, 1978). This would cause, to a fair approximation, a 20% increase in the incompatible trace elements listed in Table 5, a factor which has therefore been taken into account in inferring source composition. The model for the Bridgeman parental magma is thus much less definitive than that for Penguin Island considered above, but it should be stressed that regardless of the uncertainity in lithophile element concentrations, their relative amounts and inter-element ratios are hardly affected by this adjustment. Nevertheless, it seems likely that the source region of the Bridgeman Island volcanics is richer in Ba, Sr and especially K and Rb than that of the Penguin and, of the Deception Island basalts.

As for Penguin Island, it seems that much of the variation within the volcanics on Bridgeman Island can be explained by crystallization of the observed phenocryst phases which in this case comprise a high proportion of plagioclase felspar. This can account for the fall in Sr contents but not the positive Eu anomaly shown by the most Mg-rich basalt analysed (P.640.1b). The latter can hardly be due to cumulus plagioclase since sample P.642.2c, which has a higher proportion of plagioclase in its mode, shows no such anomaly. It seems more likely that this is a primary feature of the parent magma, caused by the exclusion of Eu^{2+} from residual clinopyroxene in the source (cf Leeman, 1976). The partitioning of Eu between clinopyroxene and basaltic liquid is dependant on oxygen fugacity (Grutzeck et al., 1974; Weill et al., 1974) and a reasonable fit with the present models would be obtained with $\log f_{O_2} \approx -12$ for P.640.1b (Bridgeman Is.) and ≈ -10 for P.721.3 (Penguin Is.). This in turn may simply reflect lower P and T in the source region of the Bridgeman Island basalts during melting compared with that of Penguin basalts.

6.3. Deception Island

Samples from Deception Island show a great range in major and trace-element geochemistry. The development of large negative Eu-anomalies (Fig. 12) shows that separation of plagioclase is a prime cause of this variability. There is evidence to suggest that this must involve low-temperature, low-pressure crystal fractionation rather than variable partial melting of a plagioclase-peridotite. Firstly, the rapid decrease in Cr and Ni contents in the andesites from the already low values in the basalts is more marked than predicted for equilibrium partial melting, except for very small degrees of melting ($\ll 1\%$) but is compatible with Rayleigh crystallisation. Secondly, the continued enrichment of the incompatible elements such as Zr and Rb with increasing SiO_2 (Fig. 11) shows that there is considerable geochemical evolution between samples such as B.107.8 and P.870.1. On the other hand, these samples have much closer total REE contents (except for Eu) which may only be reconciled if REE crystal-liquid partition coefficients were high at this stage (at least 0.3–0.5). Drake and Weill (1975) have demonstrated that partition coefficients for plagioclase are strongly temperature dependent and extrapolation of their data suggests that D_{Ce} would reach 0.3 at about 950° C. Likewise Watson (1976) has shown that REE partition coefficients increase as the liquid becomes more silicic.

The essential trace element characteristics of the Deception Island volcanics can be ascribed to the separation of plagioclase and clinopyroxene (plus olivine) from a primary magma corresponding to the most magnesian basalt (B.138.2). At least 80% solidification is necessary to account for the enrichment of the more incompatible elements (K, Rb, Zr) in the dacites, and it seems likely that this could also account for the magnitude of the Sr depletion and the Eu/Eu* ratio. Detailed calculations cannot be made because of the above reservations over the rapid increase of partition coefficients in the more evolved silicic liquids. The phenocryst assemblages are dominated by plagioclase which cannot account for the increase in Ce/Yb ratio (Table 4) with differentiation. Either fractionation in an underlying magma chamber involved a large excess of clinopyroxene which was not carried up in the lavas, or it may be that *some* of the observed chemical variation was not produced by crystal fractionation. The latter possibility receives support from the small but significant variation in $^{87}Sr/^{86}Sr$ ratios (Table 3), suggesting that the andesites may have been derived from a part of the source region slightly more enriched in Rb (and K) relative to Sr. This would also explain why the observed enrichment in incompatible elements from say B.138.2 to P.870.1 is Rb > K > Zr (Table 1).

Assuming that the chemistry of sample B.138.2 is the nearest approximation to the parental magma at Deception, this may be compared to the most primitive samples from the other two islands. The

levels of light-REE are similar to those in Penguin basalts but Zr is significantly more enriched at Deception, both of which suggest a small degree of partial melting. The relatively high heavy-REE levels show that the source is garnet-free. As at Bridgeman and Penguin, the small positive Eu-anomaly must be due to refractory clinopyroxene and excludes abundant plagioclase from the source. Thus the source mineralogy can be compared with the spinel-peridotite assumed for Bridgeman Island. Moreover, the comparison of $^{87}Sr/^{86}Sr$ ratios of volcanics from these two islands shows that their respective source regions have probably shared a similar Rb/Sr ratio for most of the Earth's history (the time-integrated value would be about 0.025). Ni and Cr contents again indicate some 20% removal of ferromagnesian minerals from a likely primary melt to produce the most primitive basalt observed and possible models F and G in Table 5 have allowed for this. The inferred trace element chemistry of the source region for 5% melting has a strong resemblance to that preferred for the Penguin basalts, particularly with regard to its low K, Rb, Sr, Ba, and Rb/Sr and its essentially flat REE patterns. The less favoured model for 10% melting requires significant enrichment in light REE relative to heavy REE but still predicts lower concentrations of K and Rb than in the Bridgeman Is. source.

The most silica-rich sample analysed from Deception Island (B.317.1) differs markedly in almost all aspects of its geochemistry from other high-silica samples (Table 1), and appears to be petrogenetically unrelated to the Deception suite. In an investigation of the geochemistry of the volcanic and plutonic calc-alkaline igneous rocks of the Antarctic Peninsula (Weaver et al., in press; Saunders et al., in press), many highly silicic rocks were encountered, similar to B.317.1, having low incompatible element (especially Zr and REE) abundances compared with rocks of intermediate compositions. It was suggested (Saunders et al., in press, Weaver et al., in press) that most of the highly silicic members of the calc-alkaline suite were generated by the fusion of sialic crustal material produced during earlier cycles of island arc magmatism. Such source material would either have to have relatively depleted incompatible element abundances or late-crystallised accessory minerals would have to be refractory, holding back Zr, REE etc.

7. Conclusions

The geochemistry of the volcanoes of Bransfield Strait displays several unusual features, some of which are indicative of island arc magmatism and others which are more typical of ocean floor basalts. Thus the high Zr/Nb, Na/K and K/Rb ratios and low Rb/Sr ratios of the basalts are characteristic of the latter. On the other hand the REE patterns are light-REE enriched ($Ce_N/Yb_N \geqq 2$) even in the most primitive basalts, and $^{87}Sr/^{86}Sr$ ratios of 0.7035 for Deception and Bridgeman lavas are much higher than in typical MORB ($\leqq 0.7030$). Alkali-silica and AFM plots (Figs. 6 and 7) suggest calc-alkaline affinities, as do the moderately high Ba and Sr contents of the lavas, yet the low Rb contents are similar to the levels in island arc tholeiites. The decoupling of many major-trace element and even trace-trace element relationships implies complexities in the source regions and in the processes of magma generation. This is perhaps not unexpected considering that the magmas were being produced during the initial stages of back-arc diapirism in an environment where island arc volcanism (and plutonism) along the margin of the Antarctic Peninsula had been actively taking place during the previous 100 m.y. or so. The inter-element plots (Fig. 11) and the associated model calculations nevertheless suggest that the source regions of all the Bransfield Strait volcanics share many geochemical features.

Modelling suggests that the primary Deception and Bridgeman magmas, generated close to the axis of back-arc spreading, last equilibrated with mantle at relatively shallow depths (< 80 km) whereas the off-axis Penguin magmas were generated at greater depth from a garnet-bearing source. In terms of $^{87}Sr/^{86}Sr$ ratios, all the Bransfield Strait lavas are more radiogenic than their Rb/Sr ratios can explain, and it is difficult to assess the extent to which depletion/enrichment processes associated with subduction and volcanism during the previous 100 m.y. or more may have upset the Rb/Sr – $^{87}Sr/^{86}Sr$ systematics. Penguin lavas are the most radiogenic, but have very low Rb/Sr: this cannot however be explained by residual phlogopite in the source. The lavas of Bridgeman and Deception have similar Ce_N/Yb_N ratios and the same $^{87}Sr/^{66}Sr$ ratios, but Bridgeman lavas have much higher K, Rb, Ba and Rb/Sr ratios despite the larger degree of partial melting predicted by the modelling. We suspect this may be due to short term metasomatic enrichment of K, Rb, and Ba in the source regions of Bridgeman magmas, possibly accompanying the dehydration of the subducting slab. Such a process has previously been invoked to explain some geochemical and isotopic features of the island arc tholeiite lavas of the South Sandwich Island Arc (Hawkesworth et al., 1977) and of the basalts of the associated back-arc spreading centre (Saunders and Tarney, in press). The entry of water into the source regions of Bridgeman magmas would allow the much greater degree of partial melting necessary to explain the low trace element abundances of Bridgeman lavas and also account for their more siliceous and high-alumina

compositions. These features are also duplicated by basalts recovered on Dredge 24 from the South Sandwich back-arc spreading centre (Saunders and Tarney, in press).

To what extent water may have accounted for the trend towards siliceous compositions during fractional crystallisation of Deception magmas is difficult to assess. Certainly, termination of an initial trend towards Fe- and Ti-enrichment occurs at an early stage. The resultant rhyodacite lavas, with high Zr and REE levels, are quite unlike equivalent calc-alkaline lavas and plutons from the Antarctic Peninsula (Saunders et al., in press; Weaver et al., in press) but closely resemble plagiogranites dredged from the ocean floor and found in ophiolite complexes (Coleman and Peterman, 1975; Saunders et al., 1979). The main difference is that plagiogranites have anomalously low K, Rb, and Ba contents, attributed to leaching with sea-water in hydrothermal convection cells, either during the final magmatic stage or closely following solidification (Saunders et al., 1979). Deception rhyodacites have not however suffered loss of these elements (although Na/K ratios are still high), probably because they have evolved in sub-aerial rather than submarine conditions.

Acknowledgements. We wish to thank the British Antarctic Survey and the Royal Navy, in particular the captains and crews of RRS Biscoe, RRS Bransfield and HMS Endurance, for logistic support in the South Shetland Islands. Dr. P.E. Baker kindly donated 14 samples and the British Antarctic Survey a further 30 samples of Deception Island lavas. Microprobe facilities were provided by the Department of Geology, University of Leicester. The financial support of the Natural Environment Research Council (Grant GR3/2993) and the University of Birmingham is gratefully acknowledged.

References

Ashcroft, W.A.: Crustal structure of the South Shetland Islands and Bransfield Strait. Brit. Antarct. Surv. Sci. Rept. **66**, 1–43 (1972)

Baker, P.E.: The South Sandwich Islands: II. Petrology and Geochemistry. Brit. Antarct. Surv. Sci. Rept. **93**, 1–34 (1978)

Baker, P.E., McReath, I., Harvey, M.R., Roobol, M.J., Davies, T.G.: The geology of the South Shetland Islands: V. Volcanic evolution of Deception Island. Brit. Antarct. Surv. Sci. Rept. **78**, 1–81 (1975)

Barker, P.F.: The tectonic framework of Cenozoic volcanism in the Scotia Sea Region – A review. In: Andean and Antarctic Volcanology Problems (O. Gonzalez-Ferran, ed.) 330–346, Rome: IAVCEI 1976

Barker, P.E., Burrell, J.: The opening of Drake Passage. Mar. Geology **25**, 15–34 (1977)

Barker, P.E., Griffiths, D.H.: The evolution of the Scotia Ridge and Scotia Sea. Phil. Trans. Roy. Soc. London, Ser. A. **271**, 151–183 (1972)

Brown, G.M., Holland, J.G., Sigurdsson, H., Tomblin, J.F., Arculus, R.J.: Geochemistry of the Lesser Antilles volcanic island arc. Geochim. Cosmochim. Acta **41**, 785–801 (1977)

Carmichael, I.S.E.: The petrology of Thingmuli, a Tertiary volcano in eastern Iceland. J. Petrol. **5**, 435–460 (1964)

Coleman, R.G., Peterman, Z.E.: Oceanic plagiogranite. J. Geophys. Res. **80**, 1099–1108 (1975)

Davey, F.J.: Marine gravity measurements in Bransfield Strait and adjacent areas. In: Antarctic Geology and Geophysics (R.J. Adie, ed.), 39–45, Oslo: Universitetsforlaget 1972

Drake, M.J., Weill, D.F.: The partition of Sr, Ba, Ca, Y, Eu^{2+}, Eu^{3+} and other REE between plagioclase feldspar and magmatic silicate liquid: an experimental study. Geochim. Cosmochim. Acta **39**, 689–712 (1975)

Erlank, A.J., Kable, E.J.D.: The significance of incompatible elements in Mid-Atlantic Ridge basalts from 45° N with particular reference to Zr/Nb. Contrib. Mineral. Petrol. **54**, 281–291 (1976)

Flower, M.F.J., Schmincke, H.-U., Thompson, R.N.: Phlogopite stability and the $^{87}Sr/^{86}Sr$ step in basalts along the Reykjanes Ridge. Nature **254**, 404–406 (1975)

Gast, P.W.: Trace element fractionation and the origin of tholeiitic and alkaline magma types. Geochim. Cosmochim. Acta **32**, 1057–1086 (1968)

Gonzalez-Ferran, O., Katsui, Y.: Estudio entegral del volcanismo Cenozoico Superior de las Islas Shetland del Sur, Antarctica. Inst. antart. chil. Ser. cient. **1**, 123–174 (1970)

Grutzeck, M., Kridelbaugh, S., Weill, D.: The distribution of Sr and REE between diopside and silicate liquid. Geophys. Res. Lett. **1**, 273–275 (1974)

Hanson, G.N.: Geochemical evolution of the suboceanic mantle. J. Geol. Soc. London **134**, 235–253 (1977)

Hart, S.R., Davis, K.E.: Nickel partitioning between olivine and silicate melt. Earth Planet. Sci. Lett. **40**, 203–219 (1978)

Hawkes, D.D.: The Geology of the South Shetland Islands, II. The geology and petrology of Deception Island. Sci. Rept. Falkland Is. Dependencies Survey **27**, 1–43 (1961)

Hawkesworth, C.J., O'Nions, R.K., Pankhurst, R.J., Hamilton, P.J., Evenson, N.M.: A geochemical study of island-arc and back-arc tholeiites from the Scotia Sea. Earth Planet. Sci. Lett. **36**, 253–262 (1977)

Hayes, D.E., Ewing, M.: Pacific boundary structure. In: The Sea (A.E. Maxwell, ed.), 29–72. New York: Wiley-Interscience 1970

Herron, E.M., Tucholke, B.E.: Sea-floor magnetic patterns and basement structure in the south eastern Pacific. In: C.O. Hollister, C. Craddock et al., Initial Rept. Deep Sea Drilling Project, 35, Washington (U.S. Government Printing Office), 263–278 (1976)

Hooker, P.J., O'Nions, R.K., Pankhurst, R.J.: Determination of rare earth elements in USGS standard rocks by mixed-solvent ion exchange and mass spectrometric isotope dilution. Chem. Geol. **16**, 189–196 (1975)

Irvine, T.N., Baragar, W.R.A.: A guide to the chemical classification of the common volcanic rocks. Can. J. Earth Sci. **8**, 523–548 (1971)

Jakobsson, S.P.: Chemistry and distribution pattern of recent basaltic rocks in Iceland. Lithos **5**, 365–386 (1972)

Karig, D.E.: Origin and development of marginal basins in the western Pacific. J. Geophys. Res. **76**, 2542–2561 (1971)

Kempe, D.C.: Petrological studies on DSDP Leg 34 basalts: Nazca Plate, Eastern Pacific Ocean. In: R.S. Yeats, S.R. Hart et al., Initial Rept. Deep Sea Drilling Project, 35, Washington (U.S. Government Printing Office) 189–213 (1976)

Kuno, H.: Lateral variation of basalt magma across continental margins and island arcs. Geol. Surv. Can. Paper **66-15**, 317–336 (1966)

Kuno, H.: Differentiation of basalt magmas. In: Basalts. (H.H. Hess and A. Poldervaart, eds.), **2**, 623–688. New York: Wiley 1968

Leeman, W.P.: Partitioning of Ni and Co between olivine and

basaltic liquid: an experimental study. Trans. Am. Geophys. Union **54**, 1222 (1973)

Leeman, W.P.: Petrogenesis of McKinney (Snake River) olivine tholeiite in light of rare-earth element and Cr/Ni distributions. Geol. Soc. Am. Bull. **87**, 1582–1586 (1976)

Lewis, J.F.: Petrology of ejected plutonic blocks of the Soufrière volcano, St. Vincent, West Indies. J. Petrol. **14**, 81–112 (1973a)

Lewis, J.F.: Mineralogy of the ejected plutonic blocks of the Soufrière volcano, St. Vincent: Olivine, Pyroxene, Amphibole and Magnetite paragenesis. Contrib. Mineral. Petrol. **38**, 197–220 (1973b)

Nicholls, I.A.: Petrology of Santorini Volcano, Cyclades, Greece. J. Petrol. **12**, 67–119 (1971)

O'Hara, M.J.: Geochemical evolution during fractional crystallisation of a periodically refilled magma chamber. Nature **266**, 503–507 (1977)

O'Nions, R.K., Pankhurst, R.J., Fridleifsson, I.B., Jakobsson, S.P.: Strontium isotopes and rare-earth elements in basalts from the Heimaey and Surtsey volcanic eruptions. Nature **243**, 213–214 (1973)

Pankhurst, R.J.: Open system crystal fractionation and incompatible element variations in basalts. Nature **268**, 36–38 (1977)

Pankhurst, R.J., O'Nions, R.K.: Determination of Rb/Sr and Sr^{87}/Sr^{86} ratios of some standard rocks and evaluation of X-ray fluorescence spectrometry in Rb-Sr geochemistry. Chem. Geol. **12**, 127–136 (1973)

Ringwood, A.E.: The petrological evolution of island arc systems. J. Geol. Soc. London **130**, 183–204 (1974)

Saunders, A.D., Tarney, J.: The geochemistry of basalts from a back-arc spreading centre in the East Scotia Sea. Geochim. Cosmochim. Acta (1979, in press)

Saunders, A.D., Tarney, J., Stern, C.R., Dalziel, I.W.D.: Geochemistry of Mesozoic marginal basin floor igneous rocks from Southern Chile. Geol. Soc. Am. Bull. (1979)

Saunders, A.D., Weaver, S.D., Tarney, J.: The pattern of Antarctic Peninsula plutonism. In: Antarctic Geoscience (C. Craddock, ed.), Madison: Univ. Wisconsin Press (1979, in press)

Stormer, J.C., Jr.: Calcium zoning in olivine and its relationship to silica activity and pressure. Geochim. Cosmochim. Acta **37**, 1815–1821 (1973)

Tarney, J., Saunders, A.D., Weaver, S.D.: Geochemistry of volcanic rocks from the island arcs and marginal basins of the Scotia Arc region. In: Island Arcs, Deep Sea Trenches and Back-Arc Basins. Maurice Ewing Series 1, 367–377. Am. Geophys. Union (1977)

Tarney, J., Saunders, A.D., Weaver, S.D., Donnellan, N.C.B., Hendry, G.L.: Minor element geochemistry of basalts from Leg 49, North Atlantic Ocean. In: J.R. Cann, B. Luyendyk et al., Initial Rept. Deep Sea Drilling Project, 49 Washington (U.S. Government Printing Office (1979, in press)

Watson, E.B.: Two-liquid partition coefficients: experimental data and geochemical implications. Contrib. Mineral. Petrol. **56**, 119–134 (1976)

Weaver, S.D., Saunders, A.D., Tarney, J.: Mesozoic-Cainozoic volcanism in the South Shetland Islands and the Antarctic Peninsula: geochemical nature and plate tectonic significance. In: Antarctic Geoscience (C. Craddock, ed.), Madison: Univ. Wisconsin Press (in press)

Weaver, S.D., Sceal, J.S.C., Gibson, I.L.: Trace-element data relevant to the origin of trachytic and pantelleritic lavas in the East African rift system. Contrib. Mineral. Petrol. **36**, 181–194 (1972)

Weill, D.F., McKay, G.A., Kridelbaugh, S.J., Grutzeck, M.: Modelling the evolution of Sm and Eu abundances during lunar igneous differentiation. Geochim. Cosmochim. Acta Suppl. **5**, 2, 1337–1352 (1974)

Wood, D.A., Tarney, J., Varet, J., Saunders, A.D., Bougault, H., Joron, J.L., Treuil, M., Cann, J.R.: Geochemistry of basalts drilled in the North Atlantic by IPOD Leg 49: implications for mantle heterogeneity. Earth Planet. Sci. Lett. (in press).

Received July 22, 1978/Accepted November 24, 1978